Translational Oncology 28 (2023) 101608

Contents lists available at ScienceDirect

Translational Oncology

journal homepage: www.elsevier.com/locate/tranon

Original Research

TYRO3 promotes chemoresistance via increased LC3 expression in pancreatic cancer

Kazushi Hara [a,b], Yosuke Horikoshi [b,*], Masaki Morimoto [a,*], Kazuhiro Nakaso [b], Teppei Sunaguchi [a,b], Tatsuyuki Kurashiki [b,c], Yuji Nakayama [d], Takehiko Hanaki [a], Manabu Yamamoto [a], Teruhisa Sakamoto [a], Yoshiyuki Fujiwara [a], Tatsuya Matsura [b,e]

[a] Division of Gastrointestinal and Pediatric Surgery, Department of Surgery, Faculty of Medicine, Tottori University Faculty of Medicine, Yonago, Japan
[b] Division of Biochemistry, Department of Pathophysiological and Therapeutic Science, Faculty of Medicine, Tottori University Faculty of Medicine, Yonago, Japan
[c] Division of Anesthesiology and Critical Care Medicine, Department of Surgery, Faculty of Medicine, Tottori University Faculty of Medicine, Yonago, Japan
[d] Division of Radioisotope Science, Research Initiative Center, Organization for Research Initiative and Promotion, Tottori University, Yonago, Japan
[e] Department of Nutritional Sciences, Faculty of Human Ecology, Yasuda Women's University, Hiroshima, Japan

ARTICLE INFO

Keywords:
Autophagy
Chemoresistance
Pancreatic cancer
Receptor tyrosine kinase
TYRO3

ABSTRACT

Pancreatic cancer (PC) is an aggressive malignancy with few treatment options, and improved treatment strategies are urgently required. TYRO3, a member of the TAM receptor tyrosine kinase family, is a known oncogene; however, the relationship between TYRO3 expression and PC chemoresistance remains to be elucidated. We performed gain- and loss-of-function experiments on TYRO3 to examine whether it is involved in chemoresistance in PC cells. TYRO3 knockdown decreased cell viability and enhanced apoptosis following treatment of PC cells with gemcitabine and 5-fluorouracil (5-FU). In contrast, no such effects were observed in TYRO3-overexpressing PC cells. It is known that autophagy is associated with cancer chemoresistance. We then examined effects of TYRO3 on autophagy in PC cells. TYRO3 overexpression increased *LC3* mRNA levels and induced LC3 puncta in PC cells. Inhibition of autophagy by chloroquine mitigated cell resistance to gemcitabine and 5-FU. In a xenograft mouse model, TYRO3 silencing significantly increased sensitivity of the cells to gemcitabine and 5-FU. To further investigate the involvement of autophagy in patients with PC, we immunohistochemically analyzed LC3 expression in the tissues of patients who underwent pancreatectomy and compared it with disease prognosis and TYRO3 expression. LC3 expression was negatively and positively correlated with prognosis and TYRO3 expression, respectively. Furthermore, LC3- and TYRO3-positive patients had a significantly worse prognosis among patients with PC who received chemotherapy after recurrence. These results indicated that the TYRO3-autophagy signaling pathway confers PC resistance to gemcitabine and 5-FU, and could be a novel therapeutic target to resolve PC chemoresistance.

Abbreviations

PC	pancreatic cancer
RTKs	receptor tyrosine kinases
5-FU	5-fluorouracil
LC3	microtubule-associated protein 1A/1B-light chain 3
ATG5	autophagy related gene 5
BECN1	beclin1
ACTB	actin beta
CQ	chloroquine
CA19–9	carbohydrate antigen 19–9
GAS6	growth arrest-specific 6

Introduction

Despite modest improvements in the survival rate of patients with cancer in recent years, the 5-year survival rate for pancreatic cancer (PC) remains the lowest among all cancers (9%) [1]. PC is the seventh leading cause of cancer-related deaths in both men and women worldwide, accounting for roughly 496,000 new cases and 466,000 deaths according to 2020 global statistics [2]. Early detection of PC is difficult, and it is often detected because of obstructive jaundice. In such cases,

* Corresponding authors.
E-mail addresses: horikoshiy@tottori-u.ac.jp (Y. Horikoshi), 2s.morimoto@gmail.com (M. Morimoto).

https://doi.org/10.1016/j.tranon.2022.101608
Received 13 August 2022; Received in revised form 16 December 2022; Accepted 19 December 2022
Available online 26 December 2022

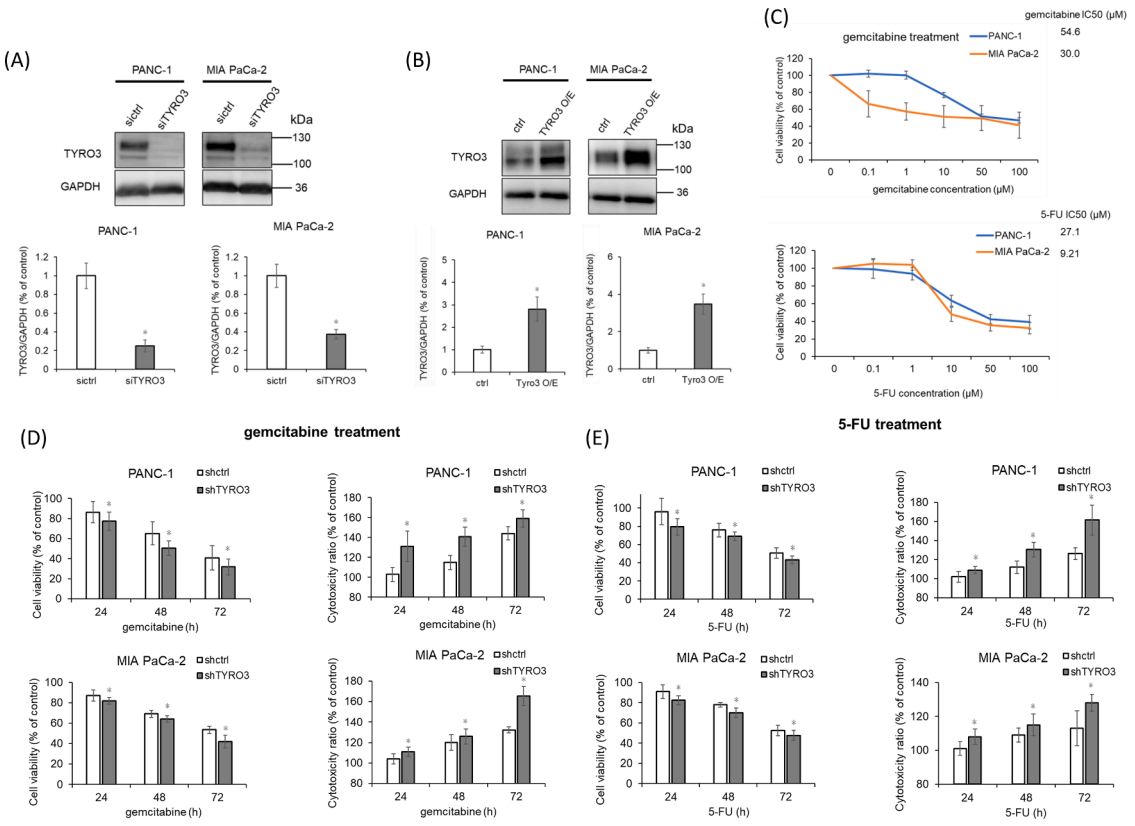

Fig. 1. TYRO3 is involved in the acquisition of chemoresistance in PC cells. (A) PANC-1 and MIA PaCa-2 cells were transfected with TYRO3 siRNA or control siRNA and analyzed using western blotting. (B) TYRO3 was overexpressed using the V5-TYRO3 plasmid in PANC-1 and MIA PaCa-2 cells and analyzed using western blotting. (C) MTT assay was performed to determine the IC50 of gemcitabine and 5-FU for 72 h in PC cells. (D and E) Cell viability and cytotoxicity in PC cells were assessed using MTT and LDH cytotoxicity assays. (D) Gemcitabine treatment. (E) 5-FU treatment. Error bars, ± standard deviation of three or six independent experiments. *$P < 0.05$ vs. control (ctrl), or shRNA control (shctrl). The concentrations of gemcitabine and 5-FU were as described in (C). TYRO3 O/E, TYRO3 overexpression; PC, pancreatic cancer; 5-FU, 5-fluorouracil; MTT, 3-(4,5-dimethyl-2-thiazolyl)−2,5-diphenyl-2H-tetrazolium bromide; LDH, lactate dehydrogenase.

percutaneous transhepatic biliary drainage or endoscopic biliary drainage is performed as a bridge to surgery and chemotherapy [3]. However, 80–85% of patients are inoperable on presentation, and most patients with PC require chemotherapy [4].

Receptor tyrosine kinases (RTKs) play an essential role in various cellular processes such as growth, survival, metabolism, and motility [5]. Molecularly targeted drugs against RTKs are used as therapeutic agents for various cancers, such as breast and ovarian cancers, with good therapeutic outcomes [6]. However, erlotinib, the only epidermal growth factor receptor tyrosine kinase inhibitor available for PC, has limited efficacy, and co-treatment with gemcitabine, a conventionally used DNA synthesis inhibitor for PC, only slightly prolongs survival [7,8]. Similarly, clinical trials using poly (ADP-ribose) polymerase (PARP) inhibitors, immune checkpoint inhibitors, agents targeting tumor metabolic pathways or tumor microenvironments, or immunotherapy in combination with standard chemotherapy including gemcitabine, produced few encouraging results [9,10]. The chemoresistance of PC seems to be attributed to the intrinsic and extrinsic characteristics of tumors, leading to a poor prognosis for patients with PC [11]. To overcome chemoresistance and improve the prognosis of patients with PC, it is essential to elucidate the underlying mechanisms and discover new molecular targets.

TYRO3, AXL, and MER, known widely as TAM receptors, were identified as new RTKs in the 1990s [12–14]. TAM receptors play critical physiological roles in cell proliferation, adhesion, and migration, as well as thrombus stabilization and inflammatory cytokine modulation [15]. Although the roles of MER and AXL in these processes have been well described, the specific functions of TYRO3 remain largely unidentified [16]. Recent studies showed that TYRO3 promotes cancer growth in bladder, breast, and colorectal cancers, hepatocellular carcinoma, and melanoma [17–21]. We previously reported that the expression of TYRO3 positively and negatively correlated with cancer growth and prognosis, respectively, in PC and gastric cancer [22,23]. TYRO3-induced chemoresistance to 5-fluorouracil (5-FU) has been reported in colorectal cancer [21]. However, the relationship between TYRO3 and chemoresistance has seen little investigation in other cancers including PC.

In the present study, we investigated the potential role of TYRO3 in regulating PC chemoresistance because both TYRO3 expression and PC resistance to chemotherapy are associated with the poor prognosis of PC. We found that TYRO3 activated autophagy via increased expression of microtubule-associated protein 1A/1B-light chain 3 (LC3), leading to gemcitabine and 5-FU resistance. Furthermore, TYRO3 expression significantly correlated with LC3 expression, and a poor prognosis in all patients with PC as well as patients who received chemotherapy after recurrence. These findings demonstrate that TYRO3 induces autophagy-mediated PC chemoresistance, and it might be a novel therapeutic molecular target in PC.

Materials and methods

Antibodies and reagents

The primary antibodies used for western blotting were as follows: anti-TYRO3 (#5585), anti-LC3B (#2775), anti-AMP-activated protein kinase α (AMPKα, #5831), anti-phospho-AMPKα (#50,081), anti-Unc-51-like kinase 1 (ULK1, #8054), anti-phospho-ULK1 (#5869), anti-regulatory-associated protein of mTOR (Raptor, #2280), anti-

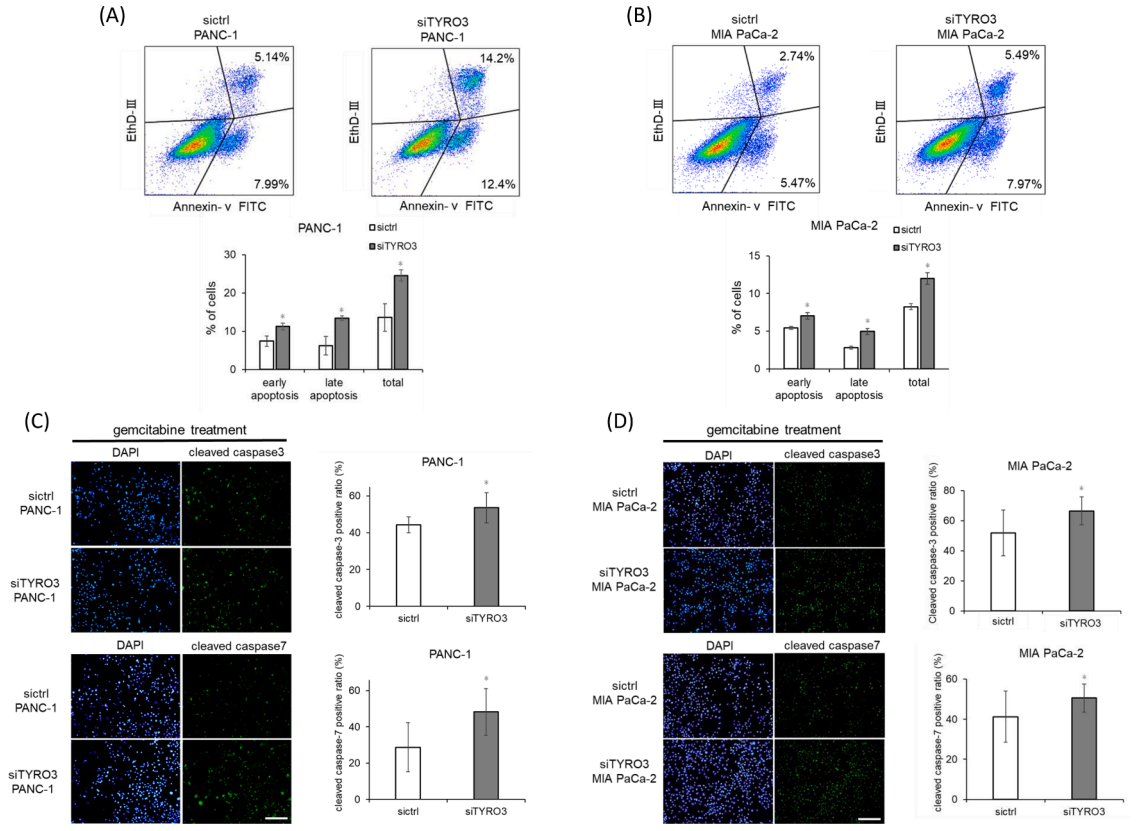

Fig. 2. TYRO3 inhibits drug-induced apoptosis in PC cells, (A and B) PC cell apoptosis induced by 24-h gemcitabine treatment was detected using flow cytometry. (C and D) Cleaved caspase 3/7 activity induced by gemcitabine for 24 h was evaluated by immunofluorescence analysis in PC cells. Scale bar, 200 μm. Error bars, ± standard deviation of three independent experiments. *$P < 0.05$ vs. siRNA control (sictrl). PC, pancreatic cancer.

phospho-Raptor (#2083), anti-Beclin (#3495), anti-phospho-Beclin (#14,717), anti-autophagy-related gene (Atg) 5 (#12,994), anti-Atg12 (#4180), anti-Atg16L1 (#8089), anti-Atg7 (#8558), anti-Atg3 (#3415) (all from Cell Signaling Technology, Danvers, MA, USA), anti-GAPDH (sc-32,233, Santa Cruz Biotechnology, Dallas, TX, USA), and horseradish peroxidase-conjugated secondary antibodies (Cytiva, Marlborough, MA, USA).

For immunofluorescence, anti-TYRO3 (#5585), anti-cleaved caspase 3 (#9664), anti-cleaved caspase 7 (#8438) (all from Cell Signaling Technology), anti-LC3 (0260–100/LC3–2G6; NanoTools, Germany), and Alexa Fluor 488-conjugated and Alexa Fluor 594-conjugated secondary antibodies (both from Thermo Fisher Scientific, Waltham, MA, USA) were used.

For immunohistochemistry, anti-TYRO3 (HPA071245; Sigma-Aldrich, St. Louis, MO, USA), anti-LC3B (NB100–2220; Novus Biologicals, Centennial, CO, USA), and anti-Ki67 (418,071; Nichirei BioScience, Tokyo, Japan) were used. Gemcitabine hydrochloride was purchased from Wako Pure Chemical Industries, Ltd. (Osaka, Japan) and Tokyo Chemical Industry Co., Ltd. (Tokyo, Japan). 5-FU and chloroquine (CQ) diphosphate salt were purchased from Sigma-Aldrich.

Cell lines and cell culture

The human PC cell lines PANC-1 and MIA PaCa-2 were purchased from the American Type Culture Collection (Manassas, VA, USA). These cells were cultured in Dulbecco's modified Eagle medium (DMEM; Nissui Pharmaceutical, Tokyo, Japan) and supplemented with 10% fetal bovine serum (FBS) and were tested negative for mycoplasma contamination (Takara Bio Inc., Shiga, Japan).

Western blotting

The methods of western blotting have been described previously [24]. Briefly, 10% or 12% SDS-PAGE was performed and the proteins were transferred to polyvinylidene fluoride (PVDF) membranes (Millipore, Billerica, MA, USA), followed by blocking with 5% skim milk for 1 h. The membranes were incubated with the appropriate primary antibody at 4 °C overnight. The next day, the washed membranes were incubated with the appropriate secondary antibody for 1 h. The signals were visualized using Immobilon Western Chemiluminescent Substrate and visualized using the Image Quant LAS 4000 mini system (GE Healthcare, Chicago, IL, USA). Quantification was performed using ImageJ (version 1.53; National Institutes of Health, Bethesda, MD, USA).

Transient overexpression and knockdown of TYRO3

For the knockdown or overexpression of TYRO3, 3–5 × 10^5 cells were seeded onto six-well plates. The methods used for the knockdown of TYRO3 have been described previously [22]. The cells were used for various assays after incubation for 24 h.

For the overexpression of TYRO3, human TYRO3 cDNA fragments were subcloned into an SRV5 vector with a 5′ V5-tag sequence [25]. The vectors were transfected using Lipofectamine 3000 (Thermo Fisher Scientific) according to the manufacturer's protocols and used for various assays after incubation for 24 h. An empty vector was employed as a control. The human TYRO3 (NM_006293) sequences were amplified by PCR (TOYOBO). The following human TYRO3 sequences were used for SRV5; Fw primer (5′-cgatatcaatggcgctgaggcggagc), Rv primer (5′-cgaattcctaacagctactgtgtggcagtagccc). For the overexpression of TYRO3 cDNA fragments were subcloned into the 5′ EcoRV and 3′ EcoRI sites of SRV5 vector with a 5′ V5-tag sequence (kindly gifted by Shigeo Ohno

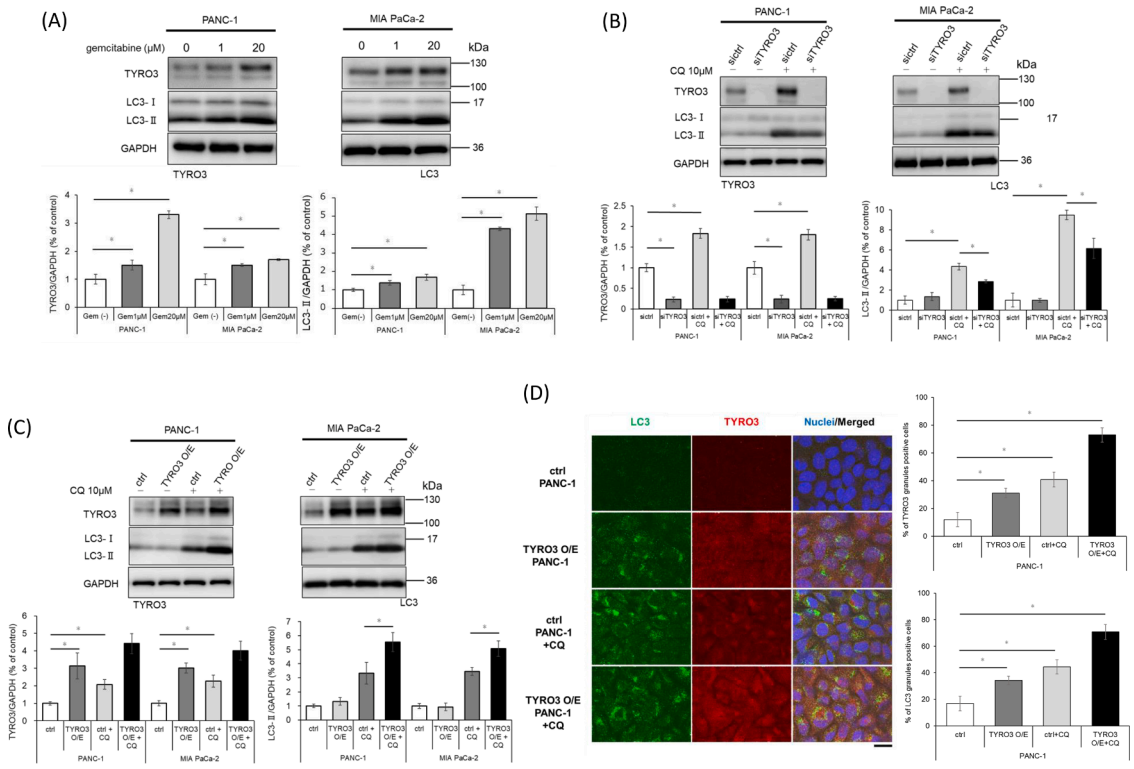

Fig. 3. TYRO3 induces LC3 expression and increases autophagosome formation in PC cells, (A) PC cells were exposed to gemcitabine for 24 h, and the expression of TYRO3 and LC3 was detected using western blotting. (B and C) The expression of TYRO3 and LC3 was examined using western blotting in TYRO3-knockdown or -overexpressing PC cells after treatment with 10 μM CQ for 24 h. (D) The expression of TYRO3 (red) and LC3 (green) were observed in TYRO3 O/E and control PC cells after treatment with 50 μM CQ for 6 h. The cells were then, fixed, permeabilized, and blocked. The cells were incubated with antibodies and obtained using a Zeiss LSM780 confocal microscope as described in Material and Methods. Scale bar, 20 μm. Error bars, ± standard deviation of 4–6 independent experiments. $*P <$ 0.05. ctrl, control; TYRO3 O/E, TYRO3 overexpression; CQ, chloroquine; PC, pancreatic cancer.

[25]), or EcoRI and blunting sites of pEGFP-C2 vector (GenBank: U57606.1).

Establishment of TYRO3 expression and knockdown stable clones

For the overexpression of TYRO3, the human TYRO3 cDNA fragment was inserted into the pEGFP-C2 vector. The vector was transfected into PANC-1 cells using Lipofectamine LTX (Thermo Fisher Scientific) and the stable clones were established as described previously [22]. The human TYRO3 (NM_006293) sequences were amplified by PCR (TOYOBO). The following human TYRO3 sequences were used for pAcGFP-N3; Fw primer (5′-cgaattcgccaccatggcgctgaggcggagc), Rv primer (5′-gcgtcgacgcacagctactgtgtggcagtagccc). For the overexpression of TYRO3 cDNA fragments were subcloned into EcoRI and blunting sites of pEGFP-C2 vector (GenBank: U57606.1).

The TYRO3-knockdown stable clones were established using lentiviruses as described previously [22]. Puromycin (Sigma-Aldrich) was used at concentrations of 0.5 μg/mL and 0.2 μg/mL for selecting PANC-1 cells and MIA PaCa-2 cells, respectively.

Cell viability assay

Cell viability was determined by 3-(4,5-dimethyl-2-thiazolyl)−2,5-diphenyl-2H-tetrazolium bromide (MTT, Dojindo Molecular Technologies, Kumamoto, Japan) assay according to the manufacturer's protocol but with slight modifications. A total of 1×10^4 tumor cells (in 100 μL) were seeded into a 96-well plate and treated with gemcitabine or 5-FU in culture medium for viability assays. After the indicated periods, the cells were treated with MTT in culture medium for 2 h at 37 °C, followed by adding 100 μL of 0.05 M HCl in 2-propanol to each well. MTT metabolism to formazan was measured using a microplate reader (Tecan, Zurich, Switzerland) at 570 nm.

Lactate dehydrogenase (LDH) cytotoxicity assay

LDH and MTT assays were performed simultaneously. After the indicated incubation period and before adding MTT reagent, 50 μL of the medium was collected and used for the LDH assay. The LDH Cytotoxicity Test wako (Wako Pure Chemical Industries) was used to measure LDH concentrations in the conditioned medium. Absorbance was measured using a microplate reader (Tecan) at 570 nm. The free LDH rate was calculated using the following equation: Free LDH rate (%) = (amount of free LDH in drug-treated cells) / (amount of free LDH in untreated controls) × 100.

Apoptosis detection assay

A total of 3×10^5 cells were seeded into a six-well plate and incubated for 24 h at 37 °C. The cells were then collected and stained using the Apoptotic/Necrotic Cells Detection Kit (PromoCell, Heidelberg, Germany) according to the manufacturer's protocol. Samples were immediately analyzed using a Gallios Flow Cytometer equipped with a 488 nm blue laser (BECKMAN COULTER Life Science, Indianapolis, IN, USA). Fluorescein isothiocyanate and ethidium homodimer III were detected using 525 nm and 620/30 nm bandpass filters, respectively. Ten thousand events were acquired and analyzed using FlowJo software (BD Biosciences, Franklin Lakes, NJ, USA).

Immunofluorescence analysis

A total of 0.5×10^5 cells were seeded onto coverslips in a 24-well plate. Gemcitabine treatment was performed for 24 h at the

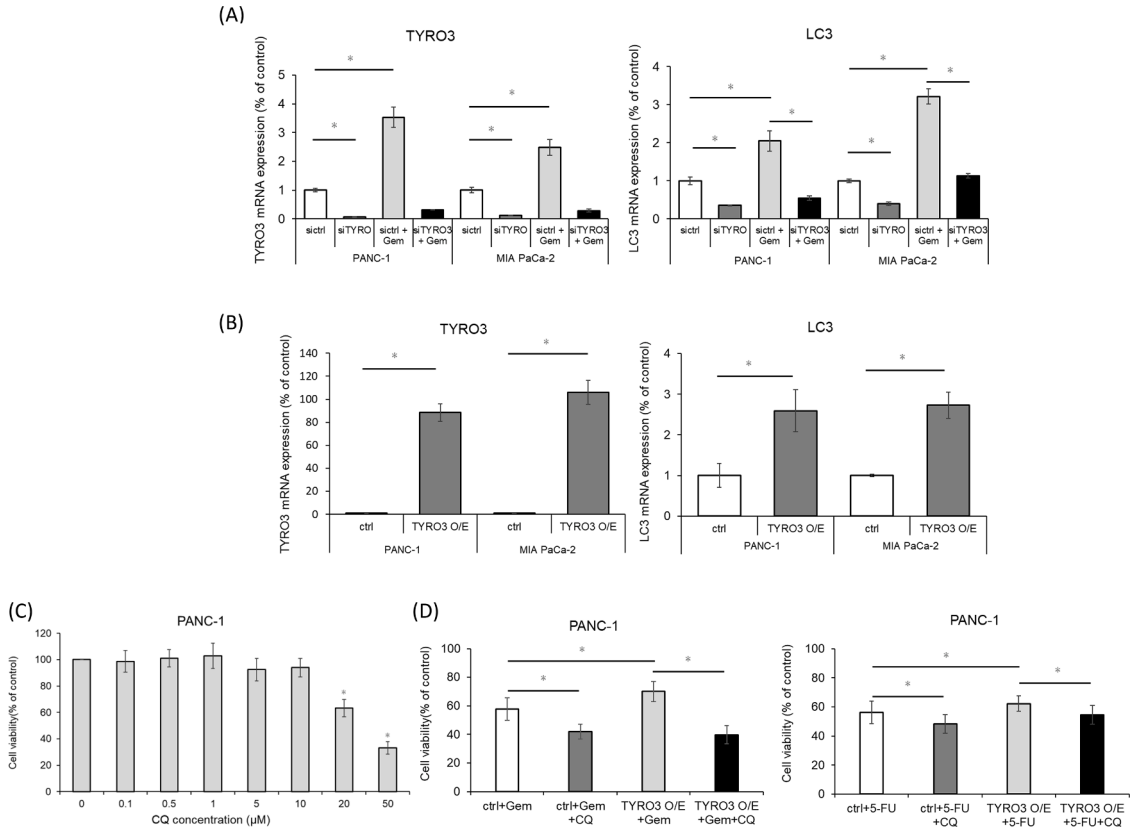

Fig. 4. TYRO3 increases LC3 mRNA levels and confers chemoresistance to PC cells, (A) Relative TYRO3 and LC3 mRNA expressions were examined using quantitative RT-PCR in TYRO3-knockdown and control PC cells undergoing gemcitabine treatment for 24 h. (B) Relative TYRO3 and LC3 mRNA expressions were examined using quantitative RT-PCR in TYRO3-overexpressing and control PC cells. (C) Cell viability was measured using MTT assay for stable TYRO3-overexpressing and control PANC-1 cells treated with gemcitabine and 5-FU for 72 h and 10 μM CQ. (D) PANC-1 cells were treated with CQ for 72 h, and cell viability was measured using the MTT assay. The cell viabilities were compared with that of 0 μM CQ. Error bars, ± standard deviation of three to six independent experiments. *$P < 0.05$. ctrl, control; TYRO3 O/E, TYRO3 overexpression; Gem, gemcitabine; CQ, chloroquine; PC, pancreatic cancer; 5-FU, 5-fluorouracil; MTT, 3-(4,5-dimethyl-2-thiazolyl)−2,5-diphenyl-2H-tetrazolium bromide.

determined concentration, and 5-FU treatment was performed for 48 h. CQ treatment was performed at a concentration of 50 μM for 6 h. The cells were then fixed with 2% paraformaldehyde in PBS, permeabilized with 0.5% Triton X-100 in PBS, and blocked with 10% FBS (fetal bovine serum) in PBS. The cells were incubated with primary antibodies overnight at 4 °C, and Alexa Fluor-conjugated secondary antibodies were used for immunostaining. Images were obtained using a conventional immunofluorescence microscope (BX53, Olympus Corp., Tokyo, Japan) to examine the expression levels of cleaved caspase 3/7 or a confocal laser scanning microscope system (LSM780; Carl Zeiss, Jena, Germany) to examine the intracellular expression levels of TYRO3 and LC3.

Colony formation assay

Cells were seeded into six-well plates at a density of 500 cells per well and incubated for 24 h at 37 °C. Gemcitabine or 5-FU treatment was performed at a predetermined concentration for 24 h. Twelve days later, the cells were fixed and stained with crystal violet.

Quantitative reverse transcription PCR

Total RNA was isolated using TRIzol reagent and the PureLink RNA Mini Kit (Thermo Fisher Scientific) according to the manufacturer's protocols. Reverse transcription was performed with 1 μg of total RNA using the SuperScript IV VILO Master Mix (Thermo Fisher Scientific). The obtained cDNAs were mixed with specific primers and Fast Advanced Master Mix (Thermo Fisher Scientific) and amplified using a ViiA 7 Real-Time PCR System (Applied Biosystems, Waltham, MA, USA) under the following conditions: 50 °C for 2 min, 95 °C for 20 s, and 40 cycles of 95 °C for 1 s and 60 °C for 20 s. Quantitative results were analyzed and are represented as fold changes. TaqMan® Gene Expression Assays (Thermo Fisher Scientific) were purchased and experiments were performed according to the manufacturer's protocol using the following primers: *TYRO3* (Hs03986773_m1), *LC3B* (Hs00797944_s1), autophagy-related gene 5 (*ATG5*, Hs00169468_m1), beclin 1 (*BECN1*, Hs01007018_m1), and actin beta (*ACTB*, Hs99999903_m1)

Subcutaneous xenograft model

Stable TYRO3 shRNA-expressing or controls cells (1×10^7) were suspended in 100 μL DMEM with 50% Matrigel (Corning Inc., Corning, NY, USA) and inoculated subcutaneously in the right dorsal side of mice (5-week-old male BALB/c nu/nu mice; CLEA Japan, Tokyo, Japan). Following tumor establishment, the mice were randomly assigned to experimental or control groups (n = 8–10 mice/group) for treatment. Depending on the groups, the mice received PBS or gemcitabine (30 mg/kg body weight, twice per week) or 5-FU (25 mg/kg body weight, twice per week) in a total volume of 200 μL PBS per injection. Tumor size was measured twice weekly using an electronic Vernier caliper, and tumor volume was calculated as follows: Volume = length × width × width/2. Mice that did not develop tumors or those that died during the experiment were excluded from the study. The mice were euthanized at the end of treatment, and the tumors were removed, weighed, and analyzed. All mouse procedures were designed and carried out according to the highest humane, scientific, and ethical principles.

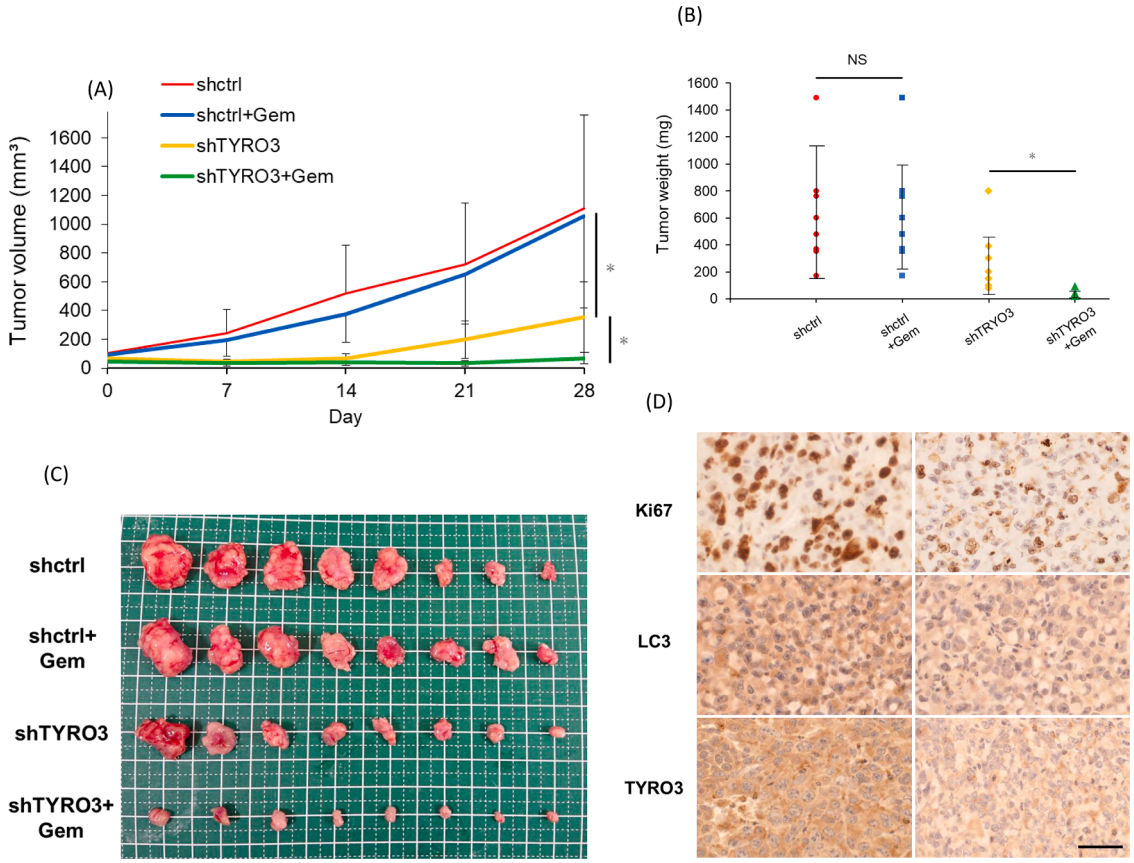

Fig. 5. TYRO3 silencing increases chemosensitivity in vivo in a mouse xenograft model of PC, (A–C) Tumor volume (A), tumor weight (B), and representative image (C) of the mice inoculated with shTYRO3-knockdown and sh-control MIA PaCa-2 cells treated with gemcitabine. (D) Histological staining of tumors using antibodies against Ki67, LC3, and TYRO3. Scale bar, 50 μm. Error bars, ± standard deviation of eight independent experiments. *$P < 0.05$. shctrl, shRNA control; Gem, gemcitabine; PC, pancreatic cancer.

Immunohistochemical staining

The methods for immunohistochemical staining have been described previously [22]. Two-tiered discrimination using positive or negative staining was used to evaluate LC3 expression in PC cells in a blinded manner. If the percentage of stained tumor cells was >10%, the sample was classified as positive. All samples were evaluated by two independent investigators (MM and KH) who were blinded to each patient's status.

Samples were obtained from 106 consecutive patients who underwent pancreatic resection at Tottori University Hospital (Yonago, Japan) for invasive pancreatic ductal carcinoma between 2006 and 2018. All patients provided informed consent and consented to pathological analysis.

Statistical analysis

Statistical analyses were conducted using "EZR" software ver1.50 or SPSS statistical software version 25.0 (IBM, Chicago, IL) [26]. Numeric data are expressed as the mean ± standard deviation of the mean, and a P-value of <0.05 was considered statistically significant. The correlations between the expression levels of LC3 and clinicopathological factors and TYRO3 identified in a previous study were analyzed using chi-square tests [22]. Continuous variables between groups were compared by one-way analysis of variance or the two-tailed Student's *t*-test. The Tukey–Kramer test was used for post-hoc analysis. Furthermore, survival curves were examined using the Kaplan–Meier method, and differences in the survival curves were compared using the log-rank test. Cox proportional hazards models were used for multivariate analysis.

Results

TYRO3 is involved in the acquisition of chemoresistance in PC cells

Previous reports have identified an increased expression of TYRO3 in tumor tissues and several types of cancer cell lines [17,21,27,28]. We have previously confirmed that TYRO3 is also expressed in PC cell lines and have reported its partial role as an oncogene [22]. This study aimed to examine whether TYRO3 is involved in chemoresistance in PC cells. We established TYRO3 overexpressing- or knockdown-PANC-1 and MIA PaCa-2 cells (Fig. 1A, B, and Supplementary Fig. 1A, B), and examined their effect on chemoresistance to gemcitabine and 5-FU. The IC50s of gemcitabine and 5-FU for PANC-1 cells were determined to be 54.6 μM and 27.1 μM, respectively, and those for MIA PaCa-2 cells were determined to be 30.0 μM and 9.2 μM, respectively (Fig. 1C). Treatment with gemcitabine and 5-FU resulted in lower viability and elevated cytotoxicity in TYRO3-suppressed cells compared with that in control cells (Fig. 1D, E). PANC-1 cells stably overexpressing TYRO3 showed increased cell viability and decreased cytotoxicity to gemcitabine and 5-FU compared to that of control cells (Supplementary Fig. 1C, D). These data imply that in PC cells, TYRO3 confers resistance against gemcitabine and 5-FU.

TYRO3 inhibits gemcitabine or 5-FU-mediated apoptosis in PC cells

Gemcitabine exerts its anticancer effect by directly or indirectly inhibiting DNA synthesis, whereas 5-FU exerts its effect through

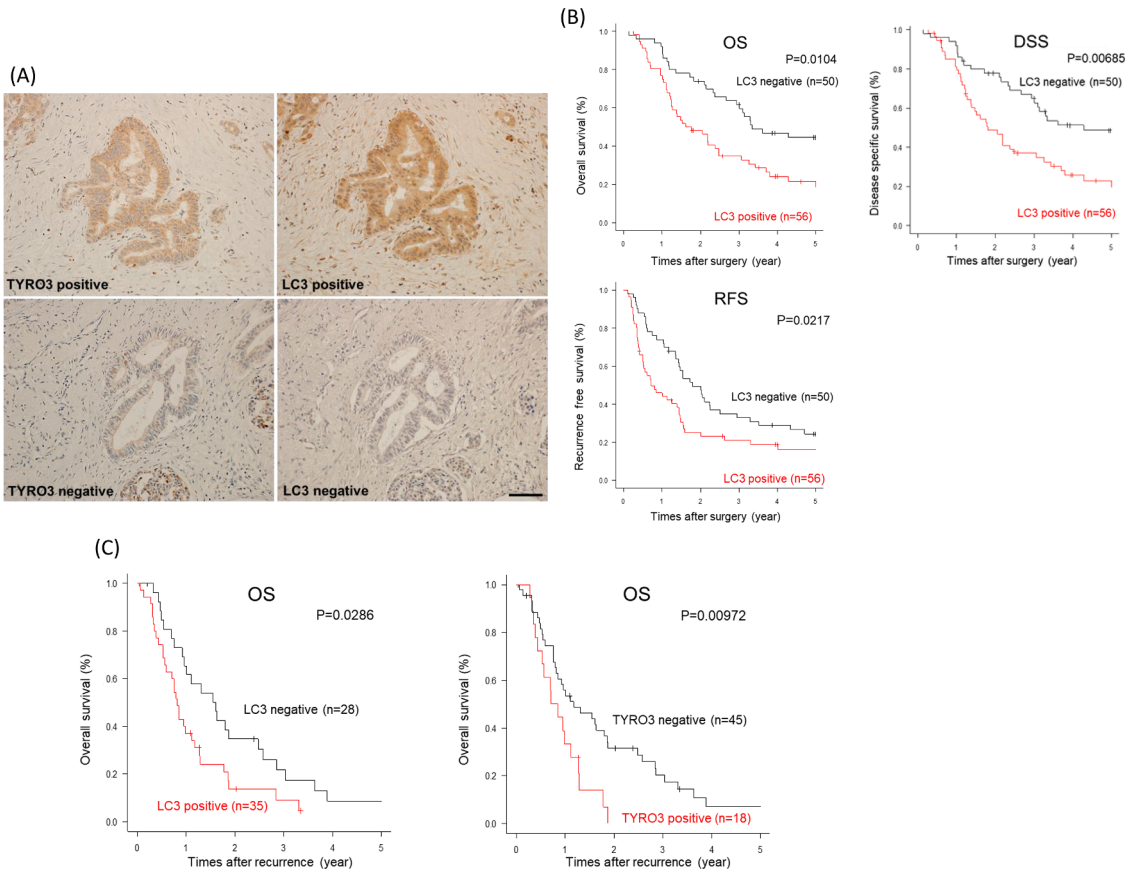

Fig. 6. Expression of LC3 in PC tissues is negatively correlated with poor prognosis of patients with PC and may be an indicator for predicting sensitivity to chemotherapy, (A) Representative images of PC tissue samples immunohistochemically stained for TYRO3 and LC3. Scale bar, 100 μm. (B) Survival curves of patients with PC stratified by LC3 expression. (C) Survival curve of patients with PC receiving chemotherapy after recurrence stratified by LC3 and TYRO3 expression. OS, overall survival; DSS, disease-specific survival; RFS, recurrence-free survival; PC, pancreatic cancer.

Table 1
Correlation analysis between LC3 and TYRO3 expressions in PC tissues using chi-square test.

	TYRO3 positive	negative	χ2	P	C
LC3					
positive	27	29	16.535	<0.001*	0.367
negative	5	45			

inhibiting thymidylate synthase and incorporating its metabolites into RNA and DNA, both resulting in cancer cell apoptosis [29,30]. We compared gemcitabine-induced cell death via apoptosis in TYRO3 knockdown cells by flow cytometry. TYRO3 knockdown itself did not exhibit apoptosis in PC cells (Supplementary Fig. 2A, B). However, gemcitabine-induced apoptosis was significantly increased in TYRO3 knockdown PC cells (Fig. 2A, B). Furthermore, apoptosis was evaluated by detecting cleaved caspase 3/7 activity using immunofluorescence. TYRO3 silencing significantly increased cleaved caspase 3/7 activity in PC cells treated with gemcitabine or 5-FU (Fig. 2C, D and Supplementary Fig. 2C, D). Treatment with gemcitabine or 5-FU decreased the colony-forming ability of TYRO3 knockdown PC cells, whereas TYRO3 overexpression enhanced their colony-forming ability (Supplementary Fig. 2E, F). These data indicate the role of TYOR3 in promoting PC cell proliferation via inhibiting gemcitabine or 5-FU-induced apoptosis.

TYRO3 induces LC3 expression and increases autophagosome formation in PC cells

Autophagy refers to the lysosomal degradation of cellular components and plays a vital role in tumor promotion, contributing to cancer cell development, proliferation, and chemoresistance. To the best of our knowledge, no studies exist on the association between TYRO3 and autophagy in PC cells; therefore, we investigated the potential role of TYRO3 in regulating autophagy by determining the levels of LC3, a widely used autophagy marker. In gemcitabine-treated PC cells, TYRO3 and LC3 expression were increased in a concentration-dependent manner (Fig. 3A). CQ is an autophagy inhibitor known to function by inhibiting lysosomal acidification [31,32]. TYRO3 silencing decreased LC3 protein levels in CQ-treated PC cells (Fig. 3B). In contrast, TYRO3 overexpression enhanced LC3 levels of the cells after CQ treatment (Fig. 3C). Both LC3 and TYRO3 puncta-positive cells were increased in TYRO3 overexpressing cells (Fig. 3D and Supplementary Fig. 3A). Furthermore, autophagy activity was tested in PC cell lines transfected with TYRO3 as well as chimeric LC3 fused with both GFP (acid--sensitive) and mCherry (acid-stable) [33]. TYRO3 overexpressing cells were positive for mCherry-LC3 puncta, indicating that autophagosomes fuse with lysosomes to form autolysosomes (Supplementary Fig. 3B). These results suggest that TYRO3 regulates autophagy in PC cells via its involvement in autophagosome and autolysosome formation.

TYRO3 increases LC3 mRNA levels and confers chemoresistance in PC cells

Autophagy is regulated by various signals generated through AMPK

Table 2
Association between LC3 expression and clinicopathological factors of all patients of PC.

		LC3 expression		P value
		Negative n = 50	Positive n = 56	
Age (years)	<65	11	11	0.814
	≧65	39	45	
Sex	Male	29	37	0.423
	Female	21	19	
BMI	<25	41	51	0.251
	≧25	9	5	
Location	Head	32	30	0.326
	Body/ tail	18	26	
Neoadjuvant chemotherapy	Yes	8	6	0.567
	No	42	50	
Adjuvant chemotherapy	Yes	30	32	0.844
	No	20	24	
Stage	I	1	5	0.21
	II/III/IV	49	51	
Histological type	well	24	23	0.617
	mod/por	23	27	
	other	3	6	
Vascular invasion	negative	5	3	0.471
	positive	45	53	
Lymphatic invasion	negative	5	5	1
	positive	45	51	
Neural Invasion	negative	1	5	0.21
	positive	49	51	
pT	I/II	2	7	0.167
	III/IV	48	49	
pN	0	22	21	0.555
	1	28	35	
Margin	0	42	48	1
	1	8	8	
CEA (ng/mL)	<5	34	28	0.0764
	≧5	16	28	
CA19–9 (U/mL)	<35	21	17	0.23
	≧35	29	39	
TYRO3 expression	positive	5	27	<0.001*
	negative	45	29	

stimulation and Atg expression [34]. TYRO3 knockdown PC cells showed no significant difference in AMPK and Atg expression (Supplementary Fig. 4A). Further, TYRO3 knockdown decreased the expression level of *LC3* mRNA in PC cells (Fig. 4A). We also observed that treatment with gemcitabine increased the mRNA level of both TYRO3 and LC3 in control PC cell lines, while gemcitabine-induced LC3 mRNA expression was suppressed in TYRO3 knockdown cells (Fig. 4A). In contrast, TYRO3 overexpression increased *LC3* mRNA expression levels in PC cells (Fig. 4B). However, TYRO3 knockdown did not affect the expression of *BECN1* and *ATG5* in PC cells (Supplementary Fig. 4B), although it was reported that *LC3, BECN1*, and *ATG5* are activated by AXL signaling [35]. These results indicate that TYRO3 signaling activates autophagy by increasing the expression of *LC3* mRNA levels. Based on these results, we tested whether the inhibition of autophagy could enhance the anticancer effect of gemcitabine or 5-FU. We found no significant decrease in cell viability upon treatment with up to 10 μM of CQ (Fig. 4C). The combination of gemcitabine or 5-FU with CQ significantly reduced cell viability compared with that of the anticancer agents alone in the PANC-1 cells and even in the TYRO3-overexpressing cells (Fig. 4D). These results suggest that TYRO3 is an upstream regulator of autophagy that promotes chemoresistance in vitro and is a potential therapeutic target.

TYRO3 confers chemoresistance in the subcutaneous xenograft mouse model of PC

To evaluate the role of TYRO3 in chemoresistance in vivo, we developed subcutaneous xenograft mouse models using TYRO3-knockdown MIA PaCa-2 cells. We found that the tumor size was significantly suppressed in the gemcitabine-treated TYRO3 knockdown cells but not in the sh-control cells (Fig. 5A). There was no difference between the groups regarding body weight (Supplementary Fig. 5A). Tumor weight analysis showed no difference between the control groups with or without gemcitabine, whereas there was a significant reduction between the TYRO3-knockdown groups (Fig. 5B, C). Treatment with 5-FU and gemcitabine showed similar results (Supplementary Fig. 5B–E). These data suggest that TYRO3 is involved in the chemotherapy resistance to gemcitabine and 5-FU. Furthermore, the expression levels of TYRO3, LC3, and Ki67 were examined using immunohistochemistry in the xenograft tissue. The expression levels of LC3 and Ki67 were positively correlated with that of TYRO3 (Fig. 5D). These results suggest that TYRO3 expression induces chemoresistance and contributes to tumor cell growth.

LC3 expression is negatively associated with prognosis in patients with PC and correlates with TYRO3 expression

To further investigate the involvement of autophagy in patients with PC, we retrospectively analyzed the expression pattern of LC3 in the tissues of 106 patients with PC and compared it with the prognosis of patients or the expression pattern of TYRO3 that we previously reported in the same cohort [22]. Immunohistochemistry analysis showed positive LC3 expression in 52.8% (56/106) of the samples, which was positively correlated with TYRO3 expression (Fig. 6A, $P < 0.001$, contingency coefficient = 0.367) (Table 1). However, no statistical differences were found between the LC3-positive and -negative groups regarding the other clinical parameters measured (Table 2). The Kaplan–Meier survival analysis demonstrated that the LC3-positive patients had significantly worse overall survival (OS), disease-specific survival (DSS), and recurrence-free survival (RFS) compared with those of the LC3-negative patients (Fig. 6B). Univariate analysis showed that, in addition to LC3, N stage and carbohydrate antigen 19–9 (CA19–9) levels were prognostic factors for OS, DSS, and RFS in patients with PC (Table 3). Multivariate analysis using the Cox proportional hazards model revealed that N stage, CA19–9 level, and LC3 expression were independent prognostic factors for OS in patients with PC (Table 4). Next, Kaplan–Meier survival analysis was performed for 63 patients who received chemotherapy after recurrence, and it revealed that LC3- and TYRO3-positive patients had significantly poorer prognosis in OS than LC3- and TYRO3-negative patients did (Fig. 6C). In contrast, clinicopathological factors demonstrated no relationship with prognosis (data not shown). Moreover, there were no statistically significant differences in background clinical parameters (Table 5). These results imply that TYRO3 expression is correlated with chemoresistance in conjunction with LC3 expression in patients with PC.

Discussion

Poor chemotherapy performance is considered one of the critical causes of the worst 5-year survival of patients with PC among all the common malignancies. Thus, expanding our understanding of PC chemoresistance could provide essential information for developing a better treatment strategy. However, the targets for overcoming chemoresistance in PC cells and their mechanisms remain largely unknown. A previous study showed TYRO3-induced 5-FU resistance in colorectal cancer; however, TYRO3-induced chemoresistance has not been reported in other cancers and with other drugs [21]. In the present study, we found that TYRO3 suppressed apoptosis induced by the anticancer drugs, gemcitabine- and 5-FU (Fig. 2). These data provide essential information to support our hypothesis that inhibition of TYRO3 may be effective in improving chemoresistance in PC.

We have previously found that TYRO3 overexpression results in increased expression of the epithelial-mesenchymal transition marker protein Snail and invasion of PANC-1 cells [22]. Overexpression of Snail

Table 3
Survival analyses of prognostic factors.

		No. patient	OS MST (days)	(95% CI)	P value	DSS MST (days)	(95% CI)	P value	RFS MST (days)	(95% CI)	P value
Age (years)	<65	22	798	401-NA	0.666	798	401-NA	0.997	508	133–1585	0.878
	≧65	84	907	749–206		1098	785–1386		524	314–570	
Sex	Male	66	850	464–1146	0.12	868	541–1222	0.35	456	227–568	0.54
	Female	40	1386	749–2171		1386	749–2171		550.5	295–770	
BMI	<25	92	1071	658–1351	0.531	866	627–1196	0.5	524	311–654	0.718
	≧25	14	1227.5	541-NA		1227.5	541–2460		438	150–561	
Location	Head	62	1071	541–1351	0.478	866	466–1351	0.876	474.5	197–540	0.0473*
	Body/tail	44	1117	798–1825		907	644–1321		568	383–962	
Neoadjuvant	Yes	14	1206	295-NA	0.61	1138.5	295-NA	0.611	552.5	137-NA	0.498
chemotherapy	No	92	972	749–1321		868	644–1196		524	295–568	
Adjuvant	Yes	62	1146	785–1982	0.394	1117	667–1386	0.38	540	314–735	0.991
chemotherapy	No	44	799	499–1321		798	429–1250		383	212–568	
Stage	I	6	1825	798-NA	0.35	1366	150-NA	0.509	1464	222-NA	0.244
	II/III/IV	100	1071	749–1321		907	644–1206		521	311–568	
Histological type	well	47	1250	868–1982	0.104	1222	907–1982	0.0555	568	493–822	0.185
	mod/ por+others	59	770	464–1190		667	429–972		314	197–540	
Vascular invasion	negative	8	2171	98-NA	0.163	2315.5	98-NA	0.243	750	89-NA	0.24
	positive	98	972	770–1250		868	644–1190		521	311–568	
Lymphatic invasion	negative	10	1982	652-NA	0.0637	1982	150-NA	0.184	654	190-NA	0.218
	positive	96	907	658–1222		866	627–1190		521	274–568	
Neural Invasion	negative	6	1115.5	160-NA	0.701	283	150-NA	0.145	1464	45-NA	0.717
	positive	100	1098	785–1321		972	770–1222		521	314–568	
pT	I/II	9	1114	406-NA	0.815	1321	150-NA	0.636	381	129-NA	0.783
	III/IV	97	1098	770–1351		907	644–1196		524	314–570	
pN	0	43	1982	1071-NA	<0.001*	1825	907-NA	0.000464*	913	524-NA	<0.001*
	1	63	658	464–1134		627	453–972		295	192–521	
Margin	0	90	1134	798–1351	0.509	972	785–1222	0.754	524	314–570	0.707
	1	16	635.5	371-NA		635.5	371-NA		421.5	217–1718	
CEA (ng/mL)	<5	62	1190	850–1566	0.265	1146	770–1564	0.241	535	381–731	0.84
	≧5	44	798	503–1206		785	450–1117		383	190–584	
CA19–9 (U/mL)	<35	38	1566	1098-NA	0.0049*	1564	1071–2460	0.0075*	750	524-NA	<0.001*
	≧35	68	770	503–1117		667	464–972		311	204–524	
LC3 expression	positive	56	658	464–907	0.00685*	616	453–907	0.0104*	295	190–528	0.022*
	negative	50	1566	1071–2625		1222	972–2171		654	498–913	

Table 4
Multivariate analysis of OS of patients with PC.

	HR	95% CI	P value
pN	2.429	1.483–3.976	<0.001*
CA19–9 (U/mL)	1.935	1.17–3.199	0.01011*
Positive LC3	1.877	1.177–2.992	0.0082*

in PANC-1 cells conferred chemoresistance to gemcitabine and 5-FU [36]. These results suggest that TYRO3 plays a crucial role in the chemoresistance of PANC-1 cells by regulating Snail expression. However, overexpression of TYRO3 in another PC cell line, MIA PaCa-2 cells, did not increase Snail expression, suggesting that the mechanism of chemoresistance requires further investigation [22]. In this study, we also analyzed the relationship between TYRO3 and clinicopathological factors such as OS, DSS and RFS in patients with PC, and we found that the expression level of TYRO3 in PC was negatively correlated with prognosis in patients with PC [22].

Recently, it has been reported that autophagy plays dual roles in tumor promotion and suppression and contributes to cancer cell development and proliferation [37]. Several studies have indicated that autophagy promotes tumor survival and growth in advanced cancers [38,39]. Han et al. reported that growth arrest-specific 6 (GAS6)-AXL signaling mediates autophagy induction by increasing the mRNA expression of *Atg5, Becn1*, and *LC3* in murine macrophages [35]. However, the molecular mechanisms of autophagy induction via TAM family proteins are not yet fully understood. LC3 is particularly critical for autophagosome formation and size regulation and is the most well-known autophagy-related molecule [40,41]. We found a positive correlation between *TYRO3* expression and *LC3* mRNA levels, despite the observation that other major autophagy signaling pathways and Atg-related proteins remained unchanged (Fig. 4A, B and Supplementary Fig. 4A). *LC3* mRNA levels were increased by gemcitabine treatment but were significantly reduced by the knockdown of TYRO3 (Fig. 4A). In addition, we found that the expression of p62/SQSTM1, another autophagy-related protein was increased in TYRO3 knockdown cells (unpublished data). It is known that autophagic degradation of p62 occurs via direct interaction with LC3 [42]. Our results suggest that the suppression of autophagy via reduction of LC3 mRNA levels by TYRO3 knockdown, caused the decrease in autophagic p62 degradation, resulting in the increase in intracellular p62. We speculate that TYRO3-related resistance to gemcitabine may involve autophagic pathway through p62/SQSTM1. These findings suggest that autophagy suppression by TYRO3 knockdown enhances drug sensitivity.

Recent evidence accounts for the improved therapeutic effects of autophagy inhibition. For example, combining an autophagy inhibitor with chemotherapy results in even greater cytotoxicity in PC cells in vitro, and the benefits of autophagy inhibition have also been shown through in vivo experiments using murine models of PC [43,44]. Moreover, clinical trials have shown that adding CQ to gemcitabine and albumin-bound (nab)-paclitaxel can improve the response rate in patients with PC [45,46]. However, autophagy inhibitors have not yet been approved as therapeutic drugs in clinical settings. It is important to note that (1) TYRO3 promotes the malignant behavior of PC cells by activating growth signaling pathways, such as PI3K/Akt and/or MEK/ERK signaling [22]; (2) TYRO3 is involved in autophagosome formation, probably via an upstream signal pathway of autophagy (Fig. 3); and (3) chemotherapy in combination with an autophagy inhibitor exhibits cytotoxic effects even in TYRO3-overexpressing PC cells (Fig. 4D). In addition, it has been reported that concurrent inhibition of

Table 5
Association between LC3 expression and clinicopathological factors of patients with PC receiving chemotherapy after recurrence.

		LC3 expression Negative n = 28	Positive n = 35	P value
Age (years)	<65	4	9	0.353
	≧65	24	26	
Sex	Male	15	25	0.0692
	Female	13	10	
BMI	<25	23	31	0.494
	≧25	5	4	
Location	Head	18	23	1
	Body/ tail	10	12	
Neoadjuvant chemotherapy	Yes	4	4	1
	No	24	31	
Adjuvant chemotherapy	Yes	22	23	0.4
	No	6	12	
Stage	I	0	3	0.247
	II/III/IV	28	32	
Histological type	well	13	12	0.63
	mod/por	14	21	
	other	1	2	
Vascular invasion	negative	1	1	1
	positive	27	34	
Lymphatic invasion	negative	2	2	1
	positive	26	33	
Neural Invasion	negative	0	3	0.247
	positive	28	32	
pT	I/II	1	5	0.214
	III/IV	27	30	
pN	0	8	11	1
	1	20	24	
Margin	0	25	33	0.648
	1	3	2	
CEA (ng/mL)	<5	22	20	0.107
	≧5	6	15	
CA19–9 (U/mL)	<35	10	9	0.421
	≧35	18	26	
TYRO3 expression	positive	2	16	<0.001*
	negative	26	19	

both ERK and autophagy signaling pathways was an effective therapeutic approach for PC [47]. Although further challenging studies are required to apply TYRO3 inhibitors and/or antibodies to everyday clinical practice, our findings that TYRO3 drives MEK/ERK as well as autophagy signaling pathways suggest that TYRO3 is a promising new molecular target with properties not found in those of existing therapeutics. Moreover, given that TYRO3 has been identified in various malignacies, it could be a common therapeutic target for a variety of cancers [16].

To truly expand our understanding of the correlations between TYRO3 expression, LC3, and patient outcomes, the surgical specimens collected from 106 patients with PC were analyzed using immunohistochemistry. LC3 has been reported to correlate with tumor stage, metastasis conditions, and the mortality of patients with PC [48]. A negative correlation between prognosis and the expression of LC3 and TYRO3 was demonstrated in patients who received chemotherapy after PC recurrence (Fig. 6C). These data suggest that TYRO3 followed by LC3 induction plays a critical role in PC prognosis and chemoresistance.

In conclusion, we demonstrated that TYRO3 induces chemoresistance in PC cells and patients with PC via LC3 induction. The TYRO3-LC3 pathway may be involved in the acquisition of resistance to the anticancer drugs gemcitabine and 5-FU. Our findings not only provide an improved prognostic marker for PC chemoresistance but also suggest a potential strategy to target TYRO3 for sensitizing PC to chemotherapy.

Funding

This work was partly supported by Tottori University's President's Discretionary Fund and Japan Society for the Promotion of Science (JSPS) KAKENHI Grant Numbers 18K10992 (T.M.), 19K07505 (Y.H.), and 20K17689 (W.M.).

Availability of data and materials

The data relating to this study are available from the corresponding author on reasonable request.

Ethics approval and consent to participate

Tissue samples and clinicopathological data were obtained from Tottori University Hospital. Our study was approved by the Institutional Review Board of Tottori University (approval number: 17A135) and was performed following the Declaration of Helsinki and its later amendments. Written informed consent was obtained from each patient. All animal experiments were approved by the Animal Care Committee of Tottori University (approval number: 20-Y-50). Mouse procedures were designed and conducted following the highest humane, scientific, and ethical principles.

Patient consent for publication

Consent was obtained in all cases.

List of Supporting Information

Supplementary Fig. 1. (A and B) The levels of TYRO3 in shTYRO3-knockdown and stable TYRO3-overexpressing PC cells were analyzed using western blotting. (C and D) Gemcitabine (C) and 5-FU (D) treatments in TYRO3-overexpressing and control PANC-1 cells. Cell viability and cytotoxicity were assessed using MTT and LDH cytotoxicity assays. Error bars, ± standard deviation of three to six independent experiments. *$P < 0.05$ vs. control (ctrl). TYRO3 O/E, TYRO3 overexpression; PC, pancreatic cancer; 5-FU, 5-fluorouracil; MTT, 3-(4,5-dimethyl-2-thiazolyl)−2,5-diphenyl-2H-tetrazolium bromide; LDH, lactate dehydrogenase

Supplementary Fig. 2. (A and B) Flow cytometric analysis of apoptosis in PC cells transfected with TYRO3 siRNA or control siRNA. (C and D) Cleaved caspase 3/7 activity induced by 5-FU for 48 h was evaluated by immunofluorescence analysis. Scale bar, 200 μm. (E and F) The colony formation ability of PC cells was assessed after treatment with gemcitabine and 5-FU. Error bars, ± standard deviation of three independent experiments. *$P < 0.05$ vs. siRNA control (sictrl). PC, pancreatic cancer; 5-FU, 5-fluorouracil

Supplementary Fig. 3. (A) The expression and localization of TYRO3 (red) and LC3 (green) were observed in TYRO3-overexpressing and control PC cells after treatment with or without 50 μM CQ for 6 h. The cells were then, fixed, permeabilized, and blocked. The cells were incubated with antibodies and obtained using a conventional immunofluorescence microscope. (B) PANC-1 cells cultured on coverslip containing dish were transfected with expression vectors encoding mCherry-GFP-LC3. After one day, the cells were subjected to a CQ treatment. At 6 h after the CQ treatment, the cells were fix and immunostained for GFP (green) and mCherry (red) to examine GFP or mCherry-positive punctures formation. A projection of the confocal sections is shown. Quantification of the number of fluorescent puncta positive cells exhibiting GFP or mCherry fluorescence. Data represent the mean ± s.d. of four independent experiments. Each photograph represents a confocal section. Scale bars: 20 μm. Statistically significant differences between the number of red and green puncta displayed by the cells are denoted by one asterisk (*) for $P<0.001$, vs ctrl mCherry-positive puncta cells, (†) for $P<0.01$, comparison with each GFP-positive puncta cells. Error bars, ± standard deviation of three independent experiments. *$P < 0.05$. ctrl, control; TYRO3 O/E, TYRO3

overexpression; CQ, chloroquine

Supplementary Fig. 4. (A) The expression of autophagy-related proteins was examined using western blotting in TYRO3-knockdown and control PC cells. (B) Relative BECN1 and ATG5 mRNA expressions were examined using quantitative RT-PCR in TYRO3-knockdown and controls PC cells treated with gemcitabine. Error bars, ± standard deviation of three independent experiments. *$P < 0.05$. ctrl, control; Gem, gemcitabine; PC, pancreatic cancer

Supplementary Fig. 5. (A) Body weights of the mice inoculated with shTYRO3-knockdown and sh-control MIA PaCa-2 cells treated with gemcitabine. (B–E) Tumor volume (B), body weight (C), tumor weight (D), and representative image (E) of the mice inoculated with shTYRO3-knockdown and sh-control MIA PaCa-2 cells treated with 5-FU. Error bars, ± standard deviation of eight to ten independent experiments. *$P < 0.05$. ctrl, control; Gem, gemcitabine; 5-FU, 5-fuorouracil

CRediT authorship contribution statement

Kazushi Hara: Conceptualization, Data curation, Formal analysis, Funding acquisition, Investigation, Methodology, Validation, Visualization, Writing – original draft, Writing – review & editing. **Yosuke Horikoshi:** Formal analysis, Funding acquisition, Project administration, Resources, Supervision, Visualization, Writing – review & editing. **Masaki Morimoto:** Conceptualization, Methodology, Project administration, Supervision, Validation, Visualization, Writing – original draft, Writing – review & editing. **Kazuhiro Nakaso:** Resources, Writing – review & editing. **Teppei Sunaguchi:** Methodology, Writing – review & editing. **Tatsuyuki Kurashiki:** Methodology, Writing – review & editing. **Yuji Nakayama:** Formal analysis, Methodology, Writing – review & editing. **Takehiko Hanaki:** Conceptualization, Methodology, Writing – review & editing. **Manabu Yamamoto:** Conceptualization, Methodology, Writing – review & editing. **Teruhisa Sakamoto:** Conceptualization, Methodology, Writing – review & editing. **Yoshiyuki Fujiwara:** Project administration, Supervision, Writing – review & editing. **Tatsuya Matsura:** Project administration, Supervision, Writing – review & editing.

Declaration of Competing Interest

The authors have no conflict of interests.

Acknowledgments

We also would like to thank Chihiro Uejima and Ken Sugezawa for insightful discussions and Wataru Miyauchi for continuous financial support. This study was partly performed using the facilities of the Tottori BioFrontier managed by the Tottori prefecture (https://www.bio-frontier.jp/english). We would like to thank Editage for English language editing (www.editage.com).

Supplementary materials

Supplementary material associated with this article can be found, in the online version, at doi:10.1016/j.tranon.2022.101608.

References

[1] C. Qin, G. Yang, J. Yang, et al., Metabolism of pancreatic cancer: paving the way to better anticancer strategies, Mol. Cancer (2020), https://doi.org/10.1186/s12943-020-01169-7.
[2] H. Sung, J. Ferlay, R.L. Siegel, et al., Global cancer statistics 2020: GLOBOCAN estimates of incidence and mortality worldwide for 36 cancers in 185 countries, CA Cancer J. Clin. (2021), https://doi.org/10.3322/caac.21660.
[3] A. Rizzo, A.D. Ricci, G. Frega, et al., How to choose between percutaneous transhepatic and endoscopic biliary drainage in malignant obstructive jaundice: an updated systematic review and meta-analysis, In vivo (2020), https://doi.org/10.21873/invivo.11964.
[4] L. Zhang, S. Sanagapalli, A. Stoita, Challenges in diagnosis of pancreatic cancer, World J. Gastroenterol. (2018), https://doi.org/10.3748/wjg.v24.i19.2047.
[5] M. Zhao, Y. Jung, Z. Jiang, et al., Regulation of energy metabolism by receptor tyrosine kinase ligands, Front. Physiol. (2020), https://doi.org/10.3389/fphys.2020.00354.
[6] T. Regad, Targeting RTK Signaling Pathways in Cancer, Cancers, Basel, 2015, https://doi.org/10.3390/cancers7030860.
[7] M.J. Moore, D. Goldstein, J. Hamm, et al., Erlotinib plus gemcitabine compared with gemcitabine alone in patients with advanced pancreatic cancer: a phase III trial of the National Cancer Institute of Canada Clinical Trials Group, J. Clin. Oncol. (2007), https://doi.org/10.1200/JCO.2006.07.9525.
[8] M. Sinn, M. Bahra, T. Liersch, et al., CONKO-005: adjuvant chemotherapy with gemcitabine plus erlotinib versus gemcitabine alone in patients after R0 resection of pancreatic cancer: a multicenter randomized phase III trial, J. Clin. Oncol. (2017), https://doi.org/10.1200/JCO.2017.72.6463.
[9] A. Di Federico, V. Tateo, C. Parisi, et al., Hacking pancreatic cancer: present and future of personalized medicine, Pharmaceuticals (2021), https://doi.org/10.3390/ph14070677.
[10] A. Di Federico, M. Mosca, R. Pagani, et al., Immunotherapy in pancreatic cancer: why do we keep failing? A focus on tumor immune microenvironment, predictive biomarkers and treatment outcomes, Cancers (2022), https://doi.org/10.3390/cancers14102429.
[11] D. Sarvepalli, M.U. Rashid, A.U. Rahman, et al., Gemcitabine: a review of chemoresistance in pancreatic cancer, Crit. Rev. Oncog. (2019), https://doi.org/10.1615/CritRevOncog.2019031641.
[12] J.P. O'Bryan, R.A. Frye, P.C. Cogswell, et al., Axl, a transforming gene isolated from primary human myeloid leukemia cells, encodes a novel receptor tyrosine kinase, Mol. Cell. Biol. (1991), https://doi.org/10.1128/mcb.11.10.5016-5031.1991.
[13] C. Lai, M. Gore, G. Lemke, Structure, expression, and Activity of Tyro 3, a Neural Adhesion-Related Receptor Tyrosine Kinase, Oncogene, 1994. https://pubmed.ncbi.nlm.nih.gov/8058320/.
[14] D.K. Graham, T.L. Dawson, D.L. Mullaney, et al., Cloning and mRNA expression analysis of a novel human protooncogene, c-mer, Cell Growth Differ. (1994). https://pubmed.ncbi.nlm.nih.gov/8086340/.
[15] M. Vouri, S. Hafizi, TAM receptor tyrosine kinases in cancer drug resistance, Cancer Res. (2017), https://doi.org/10.1158/0008-5472.CAN-16-2675.
[16] S.K. Smart, E. Vasileiadi, X. Wang, et al., The emerging role of TYRO3 as a therapeutic target in cancer, Cancers (2018), https://doi.org/10.3390/cancers10120474.
[17] F. Dufour, L. Silina, H. Neyret-Kahn, et al., TYRO3 as a molecular target for growth inhibition and apoptosis induction in bladder cancer, Br. J. Cancer (2019), https://doi.org/10.1038/s41416-019-0397-6.
[18] T.D. Kabir, C. Ganda, R.M. Brown, et al., A microRNA-7/growth arrest specific 6/TYRO3 axis regulates the growth and invasiveness of sorafenib-resistant cells in human hepatocellular carcinoma, Hepatology (2018), https://doi.org/10.1002/hep.29478.
[19] S. Zhu, H. Wurdak, Y. Wang, et al., A genomic screen identifies TYRO3 as a MITF regulator in melanoma, Proc. Natl. Acad. Sci. U.S.A. (2009), https://doi.org/10.1073/pnas.0909292106.
[20] R.C. Ekyalongo, T. Mukohara, Y. Funakoshi, et al., TYRO3 As a Potential Therapeutic Target in Breast Cancer, Anticancer Research, 2014.
[21] C.W. Chien, P.C. Hou, H.C. Wu, et al., Targeting TYRO3 inhibits epithelial-mesenchymal transition and increases drug sensitivity in colon cancer, Oncogene (2016), https://doi.org/10.1038/onc.2016.120.
[22] M. Morimoto, Y. Horikoshi, K. Nakaso, et al., Oncogenic role of TYRO3 receptor tyrosine kinase in the progression of pancreatic cancer, Cancer Lett. (2020), https://doi.org/10.1016/j.canlet.2019.11.028.
[23] C. Uejima, M. Morimoto, M. Yamamoto, et al., Prognostic significance of TYRO3 receptor tyrosine kinase expression in gastric cancer, Anticancer Res. (2020), https://doi.org/10.21873/anticanres.14572.
[24] T. Hanaki, Y. Horikoshi, K. Nakaso, et al., Nicotine enhances the malignant potential of human pancreatic cancer cells via activation of atypical protein kinase C, Biochim. Biophys. Acta (2016), https://doi.org/10.1016/j.bbagen.2016.07.008.
[25] K. Yamashita, M. Ide, K.T. Furukawa, et al., Tumor suppressor protein Lgl mediates G1 cell cycle arrest at high cell density by forming an Lgl-VprBP-DDB1 complex, Mol. Biol. Cell (2015), https://doi.org/10.1091/mbc.e14-10-1462.
[26] Y. Kanda, [Statistical analysis using freely available "EZR (Easy R)" software], Rinsho Ketsueki (2015), https://doi.org/10.11406/rinketsu.56.2258.
[27] Y. Duan, W. Wong, S.C. Chua, et al., Overexpression of Tyro3 and its implications on hepatocellular carcinoma progression, Int. J. Oncol. (2016), https://doi.org/10.3892/ijo.2015.3244.
[28] D. Chen, Q. Liu, G. Cao, et al., TYRO3 facilitates cell growth and metastasis via activation of the Wnt/β-catenin signaling pathway in human gastric cancer cells, Aging (2020), https://doi.org/10.18632/aging.102744 (Albany NY).
[29] E. Mini, S. Nobili, B. Caciagli, et al., Cellular pharmacology of gemcitabine, Ann. Oncol. (2006), https://doi.org/10.1093/annonc/mdj941.
[30] D.B. Longley, D.P. Harkin, P.G. Johnston, 5-fluorouracil: mechanisms of action and clinical strategies, Nat. Rev. Cancer (2003), https://doi.org/10.1038/nrc1074.
[31] B. Pasquier, Autophagy inhibitors, Cell. Mol. Life Sci. (2016), https://doi.org/10.1007/s00018-015-2104-y.
[32] D.J. Klionsky, A.K. Abdel-Aziz, S. Abdelfatah, et al., Guidelines for the use and interpretation of assays for monitoring autophagy (4th edition), Autophagy (2021), https://doi.org/10.1080/15548627.2020.1797280.

[33] E.N. N'Diaye, K.K. Kajihara, I. Hsieh, et al., PLIC proteins or ubiquilins regulate autophagy-dependent cell survival during nutrient starvation, EMBO Rep. (2009), https://doi.org/10.1038/embor.2008.238.
[34] B. Levine, G. Kroemer, Biological functions of autophagy genes: a disease perspective, Cell (2019), https://doi.org/10.1016/j.cell.2018.09.048.
[35] J. Han, J. Bae, C.Y. Choi, et al., Autophagy induced by AXL receptor tyrosine kinase alleviates acute liver injury via inhibition of NLRP3 inflammasome activation in mice, Autophagy (2016), https://doi.org/10.1080/15548627.2016.1235124.
[36] T. Yin, C. Wang, T. Liu, et al., Expression of snail in pancreatic cancer promotes metastasis and chemoresistance, J. Surg. Res. (2007), https://doi.org/10.1016/j.jss.2006.09.027.
[37] C.W. Yun, S.H. Lee, The Roles of Autophagy in Cancer, Int. J. Mol. Sci. (2018), https://doi.org/10.3390/ijms19113466.
[38] T. Luo, J. Fu, A. Xu, et al., PSMD10/gankyrin induces autophagy to promote tumor progression through cytoplasmic interaction with ATG7 and nuclear transactivation of ATG7 expression, Autophagy (2016), https://doi.org/10.1080/15548627.2015.1034405.
[39] M. Liu, L. Jiang, X. Fu, et al., Cytoplasmic liver kinase B1 promotes the growth of human lung adenocarcinoma by enhancing autophagy, Cancer Sci. (2018), https://doi.org/10.1111/cas.13746.
[40] E.L. Eskelinen, New insights into the mechanisms of macroautophagy in mammalian cells, Int. Rev. Cell Mol. Biol. (2008), https://doi.org/10.1016/s1937-6448(07)66005-5.
[41] Z. Xie, U. Nair, D.J. Klionsky, Atg8 controls phagophore expansion during autophagosome formation, Mol. Biol. Cell (2008), https://doi.org/10.1091/mbc.e07-12-1292.
[42] S. Pankiv, T.H. Clausen, T. Lamark, et al., p62/SQSTM1 binds directly to Atg8/LC3 to facilitate degradation of ubiquitinated protein aggregates by autophagy, J. Biol. Chem. (2007), https://doi.org/10.1074/jbc.M702824200.
[43] D. Hashimoto, M. Bläuer, M. Hirota, et al., Autophagy is needed for the growth of pancreatic adenocarcinoma and has a cytoprotective effect against anticancer drugs, Eur. J. Cancer (2014), https://doi.org/10.1016/j.ejca.2014.01.011.
[44] S. Yang, X. Wang, G. Contino, et al., Pancreatic cancers require autophagy for tumor growth, Genes Dev. (2011), https://doi.org/10.1101/gad.2016111.
[45] T.B. Karasic, M.H. O'Hara, A. Loaiza-Bonilla, et al., Effect of gemcitabine and nab-paclitaxel with or without hydroxychloroquine on patients with advanced pancreatic cancer: a phase 2 randomized clinical trial, JAMA Oncol. (2019), https://doi.org/10.1001/jamaoncol.2019.0684.
[46] H.J. Zeh, N. Bahary, B.A. Boone, et al., A randomized phase II preoperative study of autophagy inhibition with high-dose hydroxychloroquine and gemcitabine/nab-paclitaxel in pancreatic cancer patients, Clin. Cancer Res. (2020), https://doi.org/10.1158/1078-0432.ccr-19-4042.
[47] K.L. Bryant, C.A. Stalnecker, D. Zeitouni, et al., Combination of ERK and autophagy inhibition as a treatment approach for pancreatic cancer, Nat. Med. (2019), https://doi.org/10.1038/s41591-019-0368-8.
[48] L. Cui, X. Wang, X. Zhao, et al., The autophagy-related genes Beclin1 and LC3 in the prognosis of pancreatic cancer, Int. J. Clin. Exp. Pathol. (2019). http://www.ncbi.nlm.nih.gov/pmc/articles/pmc6949699/.